Eur. Phys. J. C 40, 343–347 (2005)
Digital Object Identifier (DOI) 10.1140/epjc/s2005-02138-8

THE EUROPEAN PHYSICAL JOURNAL C

Measurements of the charge asymmetry of the Dalitz plot parameters for $K^{\pm} \to \pi^{\pm}\pi^0\pi^0$ decays

G.A. Akopdzhanov, V.B. Anikeev, V.A. Bezzubov, S.P. Denisov, A.A. Durum, Yu.V. Gilitsky, S.N. Gurzhiev, V.M. Korablev, V.I. Koreshev, A.V. Kozelov[a], E.A. Kozlovsky, V.I. Kurbakov, V.V. Lipaev, V.A. Onuchin, A.M. Rybin, Yu.M. Sapunov, A.A. Schukin, M.M. Soldatov, D.A. Stoyanova, K.I. Trushin, I.A. Vasilyev, V.I. Yakimchuk, S.A. Zvyagintsev

State Research Center Institute for High Energy Physics, Protvino, Moscow oblast, 142281 Russia

Received: 2 June 2004 / Revised version: 16 January 2005 /
Published online: 3 March 2005 –

Abstract. The charge asymmetry of the g, h, and k Dalitz plot parameters for $K^{\pm} \to \pi^{\pm}\pi^0\pi^0$ decays has been measured with 35 GeV/c hadron beams at the 70 GeV IHEP accelerator. The g, h, and k values obtained appear to be identical for $K^{\pm}$ decays within the errors quoted. In particular, the charge asymmetry $A_g = (g^+ - g^-)/(g^+ + g^-)$ of the slope g is equal to $(0.2 \pm 1.9) \cdot 10^{-3}$.

PACS. 13.25.Es, 14.40.Aq

1 Introduction

The observation of direct CP violation in neutral kaon decays [1–3] motivates a search for a similar effect in charged kaon decays. CP violation, for example, could manifest itself as a charge asymmetry of the Dalitz plot parameters in $K^{\pm} \to \pi^{\pm}\pi^0\pi^0$ decays. These parameters are coefficients in a series expansion of the squared module of the matrix element [4]:

$$|M(u,v)|^2 \propto 1 + gu + hu^2 + kv^2, \qquad (1)$$

where u and v are the invariant Mandelstam variables.

Theoretical estimates of the charge asymmetry of the Dalitz plot slope g for $K^{\pm} \to \pi^{\pm}\pi^0\pi^0$ decays are uncertain and range from 10^{-6} to 10^{-3} [5–8]. In the majority of the experiments, only g^+ or g^- was measured [4,9]. From these studies it follows that $\Delta g = g^+ - g^- = 0.066 \pm 0.017$. It is very unlikely to expect direct CP violation at this level, and one can assume that the above mentioned difference is due to the underestimation of the systematic uncertainties.

$K \to 3\pi$ decays have been studied simultaneously for both K^+ and K^- mesons in [10–12]. Ford et al. [10] found $A_g = -0.0070 \pm 0.0053$ for $K^{\pm} \to \pi^{\pm}\pi^{\pm}\pi^{\mp}$ decays. Smith et al. [11] determined $A_g = 0.0019 \pm 0.0123$ for $K^{\pm} \to \pi^{\pm}\pi^0\pi^0$ decays. Preliminary analysis of our experimental data [12] based on a fraction of statistics yielded $A_g = -0.0003$ with a statistical error of 0.0025 and a systematical uncertainty below 0.0015. In this paper we report our final results on the charge asymmetry of the Dalitz plot parameter measurements.

[a] e-mail: kozelov@mx.ihep.su

2 Experimental setup

The experiment was carried out with the TNF-IHEP facility [13] (Fig. 1) at the 70 GeV IHEP accelerator. Unseparated positive and negative hadron beams with 35 GeV/c momentum are produced by 70 GeV protons in the external 30 cm Al target. The scintillation counters S1-S4 and the beam hodoscopes BH1-BH4 are used to monitor the beam intensity and to measure particle trajectories and beam profiles. The typical particle flux was $4{\times}10^6$ per 1.7 second spill.

Kaons are selected with three threshold (C1-C3) and two differential (D1,D2) gas Čherenkov counters (Fig. 1). The admixture of unwanted particles under the kaon peak was substantially below 1%. The threshold counters are also used to select 10 GeV/c electrons to calibrate the GEPARD calorimeter.

About 20% of kaons decay in the 58.5 m long vacuum pipe located downstream of the BH4 hodoscope. The flanges of the vacuum pipe have thin Mylar windows in the path of beam particles. The 3.6 m diameter exit flange is made of 4 mm thick (0.23 X_0) stainless steel. The probability of a high-energy photon to convert into an e^+e^- pair in this flange is equal to 0.16.

Kaons which pass through the decay pipe are detected by the anticoincidence counter AC. The BH5 beam hodoscope placed behind the calorimeter is used for a high precision measurement of the beam position at the setup end. The BH5 hodoscope operates in the counting mode and hence detects all beam particles.

The products of kaon decays are detected by three scintillation hodoscopes H1-H3 [14] and the GEPARD electromagnetic calorimeter. Each hodoscope is made of two X,Y

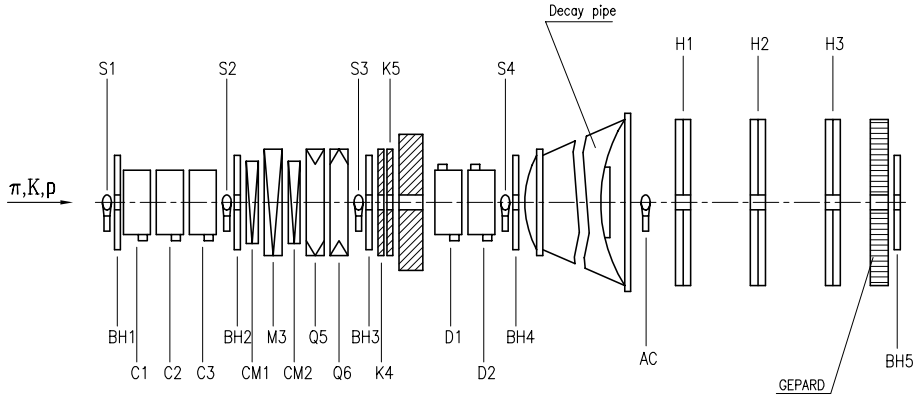

Fig. 1. Experimental layout: M – magnets, Q – quadrupoles, CM – tuning magnets, K – collimators, S – scintillation counters, C,D – threshold and differential Čherenkov counters, BH – beam hodoscopes, AC – anticoincidence counter, H – scintillation hodoscopes, GEPARD – electromagnetic calorimeter. The total length of the setup is 96 m

octagonal planes with 3.85 m distance between the opposite octagonal sides. The plane is divided into half-planes with 256 elements each. The cross section of the hodoscope elements is $14 \times 12\,\mathrm{mm}^2$ and their length varies from 0.7 to 1.8 m. Scintillation light is detected by FEU-84-3 photomultiplier tubes.

The GEPARD is a sampling lead-scintillator calorimeter. It contains 1968 cells with $76 \times 76\,\mathrm{mm}^2$ cross section. Each cell consists of 40 alternating layers of 3 mm Pb and 5 mm scintillator. The total radiation length is 21 X_0. Scintillation light is collected onto FEU-84-3 photomultiplier tubes using wavelength shifting light guides. The GEPARD calorimeter was calibrated by irradiating each cell with 10 GeV/c electrons at the beginning of data taking and by using $K^{\pm} \to \pi^{\pm}\pi^0$ reconstructed events collected during the experiment. Both methods yielded consistent results. The π^0 mass resolution is equal to $12.3\,\mathrm{MeV/c^2}$.

The Level 1 trigger is formed according to the logic formula

$$T1 = S1 \cdot S2 \cdot S3 \cdot S4 \cdot (D1 + D2) \cdot \overline{C1} \cdot \overline{C2} \cdot \overline{C3} \cdot \overline{AC}.$$

The Level 2 trigger uses information about the energy deposition in the GEPARD calorimeter [15]. For this purpose, the calorimeter is divided into 16 trigger elements. The Level 2 trigger is formed if the energy deposition exceeds 0.8 GeV in at least three trigger channels.

The stability of the beam and detector parameters was carefully monitored during the data collection. To reduce the systematic uncertainty in the measurement of the charge asymmetry of the Dalitz plot parameters, the beam polarity was reversed every day.

3 Event reconstruction and selection criteria

The $K^{\pm} \to \pi^{\pm}\pi^0\pi^0$ event selection starts by finding energy clusters in the GEPARD calorimeter. The coordinates of the cluster and the X and Y coordinates measured by the H1–H3 hodoscopes are used in track reconstruction. To reduce the combinatorial background, only tracks with three or four hits in each X and Y projection are selected. Then the vertex position of the $K^{\pm}$ decay is calculated using the reconstructed tracks. A track is considered to be associated with a kaon decay if the hypothesis of its intersection with the beam axis has a confidence level of 5% or more and the decay vertex position is inside the fiducial volume of the decay pipe. In addition, selected events have to satisfy one of the following criteria:

- five clusters with energies above 1 GeV are found and each track is associated with one of these clusters;
- four clusters with energies above 1 GeV are found and one of the tracks is not associated with these clusters.

These criteria are applied because there is a substantial probability for a gamma from π^0 decays to convert into an e^+e^- pair in the exit flange of the decay pipe (see Sect. 2), and charged pion energy depositions in the calorimeter could exceed the threshold value of 1 GeV.

Events passing this preliminary selection are subjected to a kinematic fit that allows one to resolve ambiguities due to the combinatorial background (for example in the association one of the tracks with the charged pion) and to calculate the Dalitz plot variables. Altogether 21 measured parameters are used in the fitting procedure: the energies and the coordinates of four clusters associated with gammas, the kaon mean energy and the parameters of the kaon and pion tracks. The parameters of the clusters are corrected for the transverse profile of the electromagnetic shower and for the spatial nonuniformity of the calorimeter. The energy of the charged pion is the only unknown parameter.

Seven constraints are imposed on the fitted parameters: four equations of the energy-momentum conservation, two equations for the effective masses of the gamma pairs and a required intersection of kaon and charged pion trajectories. The decay vertex coordinates are not fixed. The parameters are found by an iterative minimization of the functional using the method of Lagrange multipliers for incorporating constraints. The iterations are stopped when the relative changes of all fitted parameters at the last iteration are less than 10^{-5}. For each event all possibilities to associate one of the tracks with charged pion and γ pairs with π^0's are considered. The combination with the lowest χ^2 is used. Figure 2 shows the χ^2 distributions for the data and simulated events. Events with $\chi^2 > 20$ are rejected, since in this region the data exceeds the number of the simulated events due to the high background level. A simulation shows that this χ^2 cut decreases the background by a factor of 5, at the expence of a 28% reduced signal sample.

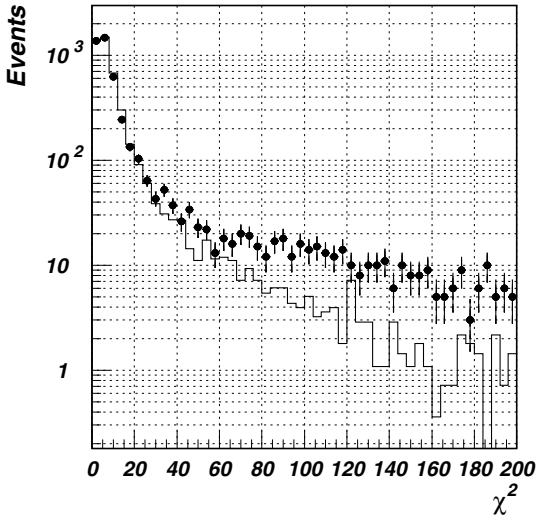

Fig. 2. χ^2 distribution for $K^\pm \to \pi^\pm\pi^0\pi^0$ decays (histogram – simulation, circles – experiment)

The experimental setup operation was simulated using a Monte Carlo (MC) method with the GEANT 3.21 code. The setup geometry is described in detail, and the data obtained in the experiment were taken into account. Among these data are the calibration coefficients for each channel of the calorimeter, the dependence of the hodoscope efficiency on the particle coordinates and correlations between kaon spatial and angular coordinates and its momentum. Figure 3 shows the acceptance of the setup, and Fig. 4 demonstrates the u, v resolutions averaged over the Dalitz plot.

The χ^2 probability $P(\chi^2)$ for data and simulation is shown in Fig. 5. Events with $P(\chi^2) > 0.1$ are selected for further analysis, since in this region there is a good agreement between the experimental and simulated data. To check the Level 2 trigger conditions, the energies corresponding to each of the trigger channels are calculated. The event is accepted if the number of the channels with energy above 1 GeV is greater than two. This cut rejects only a few $K^\pm \to \pi^\pm\pi^0\pi^0$ events (see the last row of Table 1). However, it is important for the $K^\pm \to \pi^\pm\pi^0$ event selection, which is used to calibrate the calorimeter, to adjust the simulation code, and to estimate the systematic uncertainties.

The final data sample is comprised of $N^+ = 278398$ and $N^- = 341015$ events. Table 1 shows the fraction of events rejected by each cut and the cumulative efficiency.

After applying all cuts to select $K^\pm \to \pi^\pm\pi^0\pi^0$ decays, a small admixture of background events remains. The background sources are other modes of kaon decays, interactions of beam particles in the material along the beam line and overlapping of events due to the finite time resolution of the detectors. Simulations of these processes demonstrate that the main contribution to the background comes from the $K^\pm \to \pi^\pm\pi^0$ (0.21%) and $K^\pm \to \pi^\pm\pi^+\pi^-$ (0.03%) decays. This contribution does not depend on the sign of the kaon charge and hence does not cause a false charge asymmetry of the Dalitz plots. The background level from other sources is less than 0.01%.

The finite energy resolution of the calorimeter results in a noticeable ($\sim 10\%$) probability of the wrong combinations of γ's reconstructed as π^0's and the hodoscope inefficiency can cause a reconstruction of a false track ($\sim 5\%$). Both

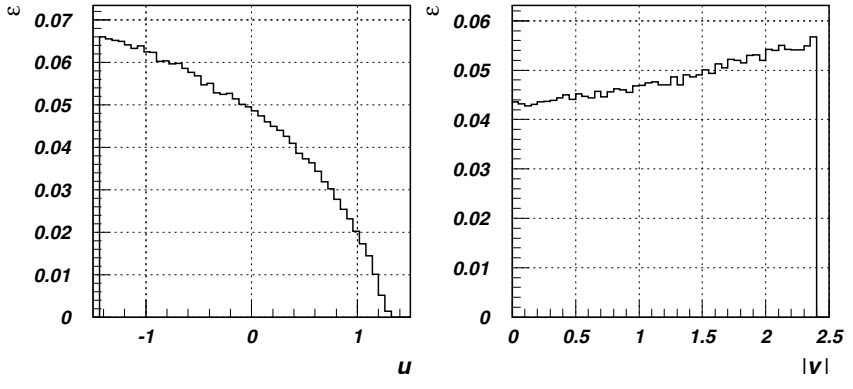

Fig. 3. Acceptance vs Dalitz plot variables

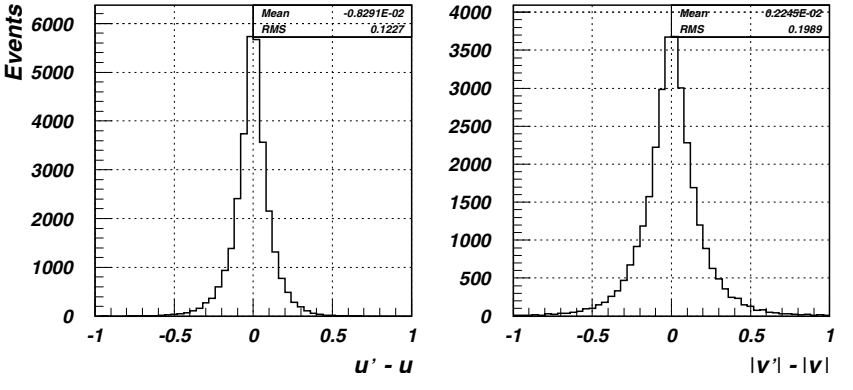

Fig. 4. u, v resolutions (u, v – "true" variables, u', v' – measured variables)

Table 1.

Selection criteria	Fraction (%) of events	
	rejected by the cut	passed this and all previous cuts
≥ 1 track is reconstructed in H1–H3	4.4	95.6
Position of the decay vertex is inside the fiducial length of the decay pipe	31.2	65.7
Number of clusters and tracks corresponds to the $K^{\pm} \to \pi^{\pm}\pi^0\pi^0$ decay	93.2	4.48
$\chi^2 < 20$	82.2	0.80
$P(\chi^2) > 0.1$	26.4	0.59
Level 2 trigger is ok	0.2	0.59

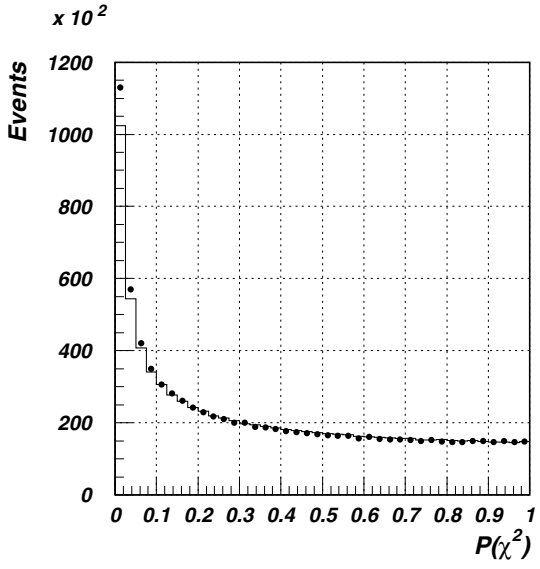

Fig. 5. $P(\chi^2)$ distribution for $K^{\pm} \to \pi^{\pm}\pi^0\pi^0$ decays (histogram – simulation, circles – experiment)

these effects are taken into account in the event simulation and it is found that their influence on the charge asymmetry of the Dalitz plot parameters is negligible.

4 Results

4.1 Difference of the Dalitz plot parameters

The difference of the Dalitz plot parameters for $K^{\pm}$ decays is estimated by minimizing the following functional form:

$$\chi^2(\Delta g, \Delta h, \Delta k) = \sum_{i,j} \frac{(r_{ij} - 1 - \alpha_{ij}\Delta g - \beta_{ij}\Delta h - \gamma_{ij}\Delta k)^2}{\sigma_{ij}^2}, \quad (2)$$

$r_{ij} = \frac{n_{ij}^+/N^+}{n_{ij}^-/N^-}$, $\sigma_{ij}^2 = r_{ij}^2 \cdot \left(\frac{1}{n_{ij}^+} + \frac{1}{n_{ij}^-}\right)$, where $n_{ij}^{\pm}$ is the number of events in the i-th, j-th Dalitz plot bin with u', v' measured coordinates, and α_{ij}, β_{ij}, and γ_{ij} are coefficients calculated by MC. The values of Δg, Δh, and Δk, as well as the elements of the correlation matrix, are:

$$\begin{cases} \Delta g = -0.0009 \pm 0.0067, \\ \Delta h = -0.0007 \pm 0.0062, \\ \Delta k = -0.0014 \pm 0.0017, \end{cases} \quad \begin{pmatrix} 1.00 & 0.93 & 0.35 \\ & 1.00 & 0.32 \\ & & 1.00 \end{pmatrix} \quad (3)$$

The errors shown are statistical only. The χ^2/ndf is $319/(279\text{-}3) = 1.16$.

Figure 6 shows the $r_i(u') = \frac{\sum_j n_{ij}^+/N^+}{\sum_j n_{ij}^-/N^-}$ and $r_j(v') = \frac{\sum_i n_{ij}^+/N^+}{\sum_i n_{ij}^-/N^-}$ ratios of the normalized event distributions in Dalitz plots for $K^{\pm} \to \pi^{\pm}\pi^0\pi^0$ decays projected on the u' and $|v'|$ axes.

Since some theoretical models predict that CP violation in $K^{\pm} \to 3\pi$ decays can be associated with the charge asymmetry of the slope g only, Δg is also estimated assuming $\Delta h = \Delta k = 0$ which is in agreement with (3). With this assumption we find:

$$\Delta g = 0.0002 \pm 0.0024, \quad \chi^2/ndf = 319/278 = 1.15. \quad (4)$$

The g, h, and k parameters appear to be equal for kaons of different charge within statistical uncertainties. However, this does not guarantee that the event distributions in the corresponding Dalitz plots are identical. In order to check the identity of u', $|v'|$, and $(u', |v'|)$ distributions independently of the assumed form of the matrix element (1), a Kolmogorov nonparametric criterion was used. This analysis provided the following results: the probabilities that u', $|v'|$ and two-dimensional $(u', |v'|)$ distributions for K^+ and K^- are indistinguishable and equal to 32.4%, 85.4% and 55.2%, respectively.

4.2 Systematic errors

All measures have been taken to assure that K^+ and K^- beams have identical parameters. Nevertheless, the average angles A_X and A_Y of beam particles with respect to the nominal beam axis and the mean kaon energies in the

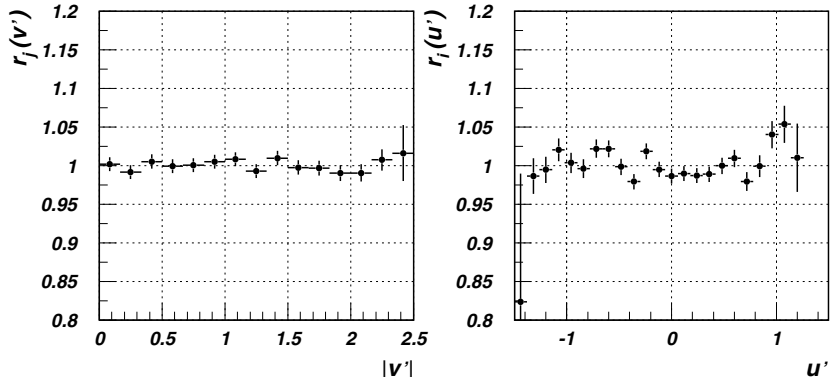

Fig. 6. Ratios of normalized event distributions projected on the u' and $|v'|$ axes

positive and negative beams could differ by $\Delta A_X = 5\,\mu rad$, $\Delta A_Y = 7\,\mu rad$ and $\Delta E = 50$ MeV. Simulations show that these uncertainties result in the following systematic errors:

$$\delta_A(\Delta g) = 0.0004, \quad \delta_A(\Delta h) = 0.0003, \quad \delta_A(\Delta k) = 0.0001,$$
$$\delta_E(\Delta g) = 0.0006, \quad \delta_E(\Delta h) = 0.0004, \quad \delta_E(\Delta k) = 0.0001.$$

Other possible sources of the systematic errors include the time variations of the calorimeter calibration coefficients and the hodoscope efficiency, the influence of the Earth magnetic field on the particle beams of different polarity, the difference in the π^+ and π^-interactions with matter, and the difference in composition and intensity of the positive and negative beams. The total contribution of these factors to the systematic errors does not exceed $1 \cdot 10^{-4}$.

We also investigated that varying the minimum energy of γ's, the minimum and maximum energies of the charged pion, the value of $P(\chi^2)$ and the number of reconstructed tracks did not appreciably change the results. The results also remain unaffected if the bins located at the boundary of the Dalitz plot are not used. Δg, Δh, and Δk can alternatively be found by minimizing the functional for the differences of the Dalitz plots. The results obtained agree with (3) and (4).

Thus, the final estimates of the systematic errors are

$$\delta(\Delta g) = 0.0007, \quad \delta(\Delta h) = 0.0005, \quad \delta(\Delta k) = 0.00014(5)$$

The systematic errors are approximately an order of magnitude smaller than the statistical errors given in (3).

Conclusions

The differences Δg, Δh, Δk of the Dalitz plot parameters have been measured for $K^\pm \to \pi^\pm\pi^0\pi^0$ decays using the TNF-IHEP facility. The studies were performed using the 35 GeV/c positive and negative hadron beams at the 70 GeV IHEP accelerator. Frequent changes of the beam polarity allowed one to minimize the systematic uncertainties of the experiment. Our results show that the event distributions in the Dalitz plots for K^+ and K^- decays are indistinguishable and that Δg, Δh, and Δk are consistent with zero within the statistical and systematic errors.

Assuming $\Delta h = \Delta k = 0$ we find:

$$\Delta g = 0.0002 \pm 0.0024(stat.) \pm 0.0007(syst.).$$

The asymmetry $A_g = \Delta g/(g^+ + g^-)$, calculated under the assumption $g^+ = g^- = 0.652$ [4], is measured to be $A_g = 0.0002 \pm 0.0018(stat.) \pm 0.0005(syst.)$.

This is the most accurate estimate of the charge asymmetry of the Dalitz plot slope for the $K^\pm \to \pi^\pm\pi^0\pi^0$ decay so far.

Acknowledgements. We are grateful to A.A. Logunov, N.E. Tyurin, and A.M. Zaitzev for their support of the experiment; to V.N. Mikhailin for his assistance in the setup construction and operation; to Yu.V. Mikhailov, A.N. Sytin, and V.A.Sen'ko for their help in manufacturing electronics. We thank the staff of the Accelerator Department and the Beam Division who provided high-quality operations of the accelerator complex, beam extraction system, and the beam channels No.8 and No.23. We appreciate the assistance of I.N. Belyakov, Yu.G. Nazarov, A.N. Romadanov, and I.V. Shvabovich in the detector construction. This study is supported in part by the Russian Fund for Basic Research (grants 02-02-17018, 02-02-17019) and the President grant 1305.2003.2.

References

1. A.J. Bevan, et al., Phys. Lett. B **465**, 355 (1999)
2. A. Lai, et al., Eur. Phys. J. C **22**, 231 (2001)
3. A. Alavi–Harati, et al., Phys. Rev. Lett. **83**, 22 (1999)
4. K. Hagiwara, et al., Phys. Rev. D **66**, 010001 (2002)
5. A.A. Belkov, et al., Czech. J. Phys. **53**, Suppl. A (2003), hep–ph/0311209
6. G. D'Ambrosio, et al., Phys. Lett. B **273**, 497 (1991)
7. G. Isidori, et al., Nucl. Phys. B **381**, 522 (1992)
8. E. Gamiz, J. Prades, I. Scimemi, J. High Energy Phys. **09**, 042 (2003)
9. I.V. Ajinenko, et al., Phys. Lett. B **567**, 159 (2003)
10. W.T. Ford, et al., Phys. Rev. Lett. **25**, 1370 (1970)
11. K.M. Smith, et al., Nucl. Phys. B **91**, 45 (1975)
12. G.A. Akopdzhanov, et al., in: Proceedings of the First International Workshop on Frontier Science – Charm, Beauty, and CP, Frascati, 2002, edited by L. Benussi, et al., (LNF, Frascati, 2002), p. 229
13. V.V. Ammosov, et al., Preprint IHEP 98-2, Protvino, 1998
14. A.V. Vasiliev, et al., Instrum. Exp. Tech. **2**, 50 (1993)
15. Yu.V. Gilitsky, et al., Preprint IHEP 93-10, Protvino, 1993